THE JOURNAL OF PHYSICAL CHEMISTRY A

Article

pubs.acs.org/JPCA

Systematic Theoretical Study of Non-nuclear Electron Density Maxima in Some Diatomic Molecules

Luiz A. Terrabuio, Tiago Q. Teodoro, Marina G. Rachid, and Roberto L. A. Haiduke*

Departamento de Química e Física Molecular, Instituto de Química de São Carlos, Universidade de São Paulo, CP 780, 13560-970 São Carlos, São Paulo, Brazil

Supporting Information

ABSTRACT: First, exploratory calculations were performed to investigate the presence of non-nuclear maxima (NNMs) in ground-state electron densities of homonuclear diatomic molecules from hydrogen up to calcium at their equilibrium geometries. In a second stage, only for the cases in which these features were previously detected, a rigorous analysis was carried out by several combinations of theoretical methods and basis sets in order to ensure that they are not only calculation artifacts. Our best results support that Li_2, B_2, C_2, and P_2 are molecules that possess true NNMs. A NNM was found in values obtained from the largest basis sets for Na_2, but it disappeared at the experimental geometry because optimized bond lengths are significantly inaccurate for this case (deviations of 0.10 Å). Two of these maxima are also observed in Si_2 with CCSD and large basis sets, but they are no longer detected as core−valence correlation or multiconfigurational wave functions are taken into account. Therefore, the NNMs in Si_2 can be considered unphysical features due to an incomplete treatment of electron correlation. Finally, we show that a NNM is encountered in LiNa, representing the first discovery of such electron density maxima in a heteronuclear diatomic system at its equilibrium geometry, to our knowledge. Some results for LiNa, found in variations in internuclear distances, suggest that molecular electric moments, such as dipole and quadrupole, are sensitive to the presence of NNMs.

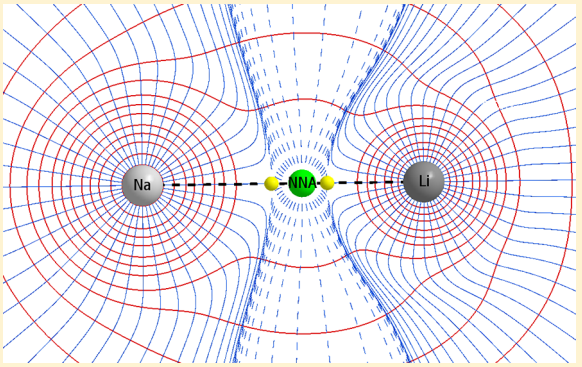

INTRODUCTION

The existence of non-nuclear maxima (NNMs) or, as also called, non-nuclear attractors (NNAs) in electron densities (ρ) of molecular systems has been cogitated since 1955, when Hartree−Fock (HF) calculations on Li_2 indicated such a possibility.[1,2] This small molecule has been subjected to a series of similar studies with increasing theoretical treatment sophistication.[2−6] Presently, electron density NNMs can be assumed as real entities because the most advanced calculation levels employed for Li_2, including full configuration interaction (CI), still support the existence of one NNM at the middle of this Li−Li bond. However, although the evidence seems definitive for Li_2, the same cannot be said for other systems in which experimental and theoretical data are still inconclusive.

NNMs have also been detected in Na_2 and clusters of lithium and sodium, suggesting that these electron density features are responsible for some properties of alkali metals.[7,8] In 1999, the promolecular model, in which the electron density of a molecule is constructed by superpositions of free atomic densities, was used to indicate homonuclear molecules more likely to present NNAs around their equilibrium geometries.[9] This model also provided an interpretation of universal features observed in electron densities during variations in internuclear distances, indicating that NNMs might be observed in certain ranges that can include the equilibrium bond length.[9,10] Thus, according to Pendás and co-workers,[9] NNAs are a direct consequence of the atomic shell structure as two atoms bind together. They indicated that the molecular electron density is nicely described by the promolecular model and that NNMs appear as maxima in atomic electron densities superimpose in space. A selection of density functionals that better describe characteristics of X-ray experiments in solid magnesium and their posterior applications to electron density studies in crystals of beryllium and magnesium have showed that NNAs are only observed in the first metal.[11] Other studies have also dealt with NNMs in metals at equilibrium volumes, and the evidence is supportive of them in lithium and beryllium.[12,13] Zhikol and co-workers pursued the answer to a possible existence of NNAs along the Si−Si bond in Si_2H_6, which is presented as the simplest laboratory system for crystal silicon.[14] After several calculations with different methods and basis sets, the authors concluded that NNMs in this Si−Si bond are unphysical and should be ascribed to a deficiency in the basis set employed. Tognetti and Joubert dealt with the use of various density functionals to describe features of bond critical points (BCPs) of approximately 50 molecules and their

Received: July 15, 2013
Revised: September 5, 2013
Published: September 10, 2013

   dx.doi.org/10.1021/jp406992q | J. Phys. Chem. A 2013, 117, 10489−10496

Table 1. Equilibrium Bond Length (r_e), Harmonic Vibrational Frequency (ω), Total Energy (E_T), Number of Non-nuclear Attractors (NNAs), Atomic Charges (q_i), Densities at BCPs and NNAs (ρ), and the Distance between the Nearest Atom and the NNA (r_{NNA}) for the Li_2 Molecule (Singlet State)[a]

	CCSD								CCSD(FU)	CAS[b]	
	DZ	TZ	a-TZ	u-TZ	QZ	a-QZ	u-QZ	5Z-mod	CVQZ	DZ	exp[6,46]
r_e (Å)	2.7284	2.7006	2.6999	2.6993	2.6984	2.6987	2.6984	2.6984	2.6729[c]	2.6729[c]	2.6729
ω (cm^{-1})	340.4	344.7	344.9	346.3	346.6	346.3	346.6	346.6	–	–	351.4
$-E_T$(H)	14.9006	14.9032	14.9034	14.9035	14.9037	14.9037	14.9037	14.9038	14.9907	14.9014	14.9949
NNAs	1	1	1	1	1	1	1	1	1	1	
q_{Li} (e)	0.587	0.628	0.630	0.627	0.634	0.634	0.633	0.627	0.622	0.592	
q_{NNA} (e)	−1.174	−1.257	−1.260	−1.255	−1.269	−1.270	−1.267	−1.255	−1.245	−1.184	
ρ_{NNA} (au)	0.01249	0.01356	0.01360	0.01366	0.01382	0.01382	0.01383	0.01378	0.01421	0.01284	
ρ_{BCP} (au)	0.01165	0.01266	0.01269	0.01278	0.01287	0.01287	0.01289	0.01292	0.01331	0.01203	
r_{NNA} (Å)	1.3642	1.3503	1.3500	1.3497	1.3492	1.3494	1.3492	1.3492	1.3365	1.3365	

[a]XZ = cc-pVXZ, a-XZ = aug-cc-pVXZ, u-XZ = uncontracted cc-pVXZ, CVXZ = cc-pCVXZ, and 5Z-mod = cc-pV5Z modified. [b]CAS-SCF(6,28). [c]Calculation performed at the experimental geometry.

comparison with results from wave-function-based methods, such as HF, perturbation theory (MP2), and coupled cluster theory (CCSD).[15] This article discusses that a NNA is found for Li_2 with all density functional theory (DFT) variants studied. However, the DFT methods are not capable of finding NNMs in Na_2, though they can be observed with the other theoretical treatments employed as references. In the case of Si_2, the authors show that HF predicts only one NNA, CCSD furnishes two NNMs, and MP2, along with all functionals, provides no NNA at all. Finally, one NNM was observed for P_2 with all methods except SVWN, PBE, and BLYP.[15]

There are some studies that also investigated the existence of NNMs in solid-state heterocompounds. Platts and Bader removed a fluorine atom in a cubic $Li_{14}F_{13}^+$ cluster and found that F centers are associated with NNAs.[16] Another work revealed that reliable experimental evidence of NNAs is found in a dimeric magnesium compound.[17] However, NNAs in heteronuclear diatomic molecules are considered exceptional features independently of the internuclear distance analyzed.[9] This indicates that diatomic heteronuclear systems that exhibit NNMs at equilibrium distances must be extremely rare, and no example was ever observed as far as we know.

Our objective is to study the possible existence of true NNMs in ground-state electron densities of homonuclear diatomic molecules from hydrogen up to calcium at their equilibrium geometries. Reliable methods including electron correlation are employed here as single reference coupled cluster theory considering single and double excitations (CCSD), along with complete active space multiconfiguration self-consistent field (CAS-SCF) and the restricted active space variation (RASSCF). The basis sets used vary from cc-pVDZ to a modified version of cc-pV5Z, including some decontracted basis sets and choices with diffuse (aug) or core−valence correlation (CV) functions. Quantities derived from the quantum theory of atoms in molecules (QTAIM)[18,19] are discussed to fully characterize the properties of basins associated with NNAs. Finally, we also seek NNMs in a heteronuclear diatomic molecule, LiNa.

CALCULATION DETAILS

Electronic structure calculations were performed by Gaussian 03.[20] Almost all investigations employed the frozen-core (FC) version of the theoretical method except when clearly indicated by a label referring to the full (FU) variant. Quantities were obtained here by the use of generalized densities. The analysis of electron density features was carried out by the QTAIM algorithm implemented in Gaussian 03[21−34] and AIMALL,[35] whenever a first attempt with Gaussian 03 did not furnish all of the QTAIM quantities required.

Moreover, cc-pVDZ, cc-pVTZ, aug-cc-pVTZ, cc-pVQZ, aug-cc-pVQZ, cc-pV5Z, and cc-pCVQZ basis sets[36−42] were considered in our study. The modified version of the cc-pV5Z basis set, referred to here as cc-pV5Z-mod, was obtained by a simple removal of those functions associated with the largest angular momentum value of each atom. Exploratory calculations for K_2 employed the Feller Misc. CVQZ basis set.[43] Basis sets not included in Gaussian 03 were taken from EMSL.[44,45] Finally, uncontracted sets are labeled here as u-cc-pVXZ (X = T or Q).

RESULTS AND DISCUSSION

Homonuclear Systems. Investigative exploratory calculations were performed at optimized or experimental geometries[46−48] by means of the CCSD method and a quadruple-ζ basis set (Feller Misc. CVQZ for potassium and cc-pVQZ for the remaining atoms). Some data from this previous study can be found in Table S1 (Supporting Information). The analysis pointed to evidence of NNAs in Li_2, B_2, C_2, Na_2, Si_2, and P_2.

Table 1 shows all of the values obtained for Li_2. Calculations performed in this molecule support a single NNM located at the middle of such Li−Li bond. The results from CCSD(FC) with different basis sets show a clear convergence pattern for quantities calculated, and the deviations found between those values obtained with quadruple-ζ variants and cc-pV5Z-mod are within 0.026 Å and 5 cm^{-1} of experimental data[46] for equilibrium bond lengths (r_e) and harmonic vibrational frequencies (ω), respectively. Data from the exact CAS-SCF(6,28) method with a cc-pVDZ set also agree with the same overall description given by CCSD. The inclusion of CV with specific basis sets, CCSD(FU)/cc-pCVQZ, furnishes a much better total energy value and provides again one NNM (certainly, FU calculations done also include some core−core correlation, but this effect should be negligible because appropriate basis sets to deal with such aspect were not used here). It is important to compare electron density values at BCPs to those at NNAs. We found that these densities also converge nicely with basis set increments, and the difference between ρ_{NNA} and ρ_{BCP} is approximately equal to 0.001 au according to our best predictions, in nice agreement with other accurate values from the literature.[6]

dx.doi.org/10.1021/jp406992q | J. Phys. Chem. A 2013, 117, 10489−10496

Table 2. Equilibrium Bond Length (r_e), Harmonic Vibrational Frequency (ω), Total Energy (E_T), Number of Non-nuclear Attractors (NNAs), Atomic Charges (q_i), Densities at BCPs and NNAs (ρ), and the Distance between the Nearest Atom and the NNA (r_{NNA}) for the B_2 Molecule (Triplet State)[a]

	CCSD								CCSD(FU)	CAS[b]	
	DZ	TZ	a-TZ	u-TZ	QZ	a-QZ	u-QZ	5Z-mod	CVQZ	QZ	exp[46]
r_e (Å)	1.6292	1.6033	1.6032	1.6008	1.5969	1.5971	1.5977	1.5959	1.590[c]	1.590[c]	1.590
ω (cm^{-1})	1008.6	1029.8	1027.9	1032.5	1037.6	1037.0	1035.0	1038.1	–	–	1051.3
$-E_T$(H)	49.2572	49.2790	49.2800	49.2811	49.2861	49.2865	49.2864	49.2875	49.3850	49.1900	
NNAs	0	1	1	1	2	2	2	2	2	0	
q_B (e)	0	0.444	0.440	0.450	0.463	0.468	0.473	0.456	0.472	0	
q_{NNA} (e)	–	−0.890	−0.882	−0.901	−0.464	−0.469	−0.474	−0.457	−0.473	–	
ρ_{NNA} (au)	–	0.1380	0.1382	0.1392	0.1411	0.1410	0.1409	0.1414	0.1427	–	
ρ_{BCP1} (au)[d]	–	0.1365	0.1368	0.1377	0.1404	0.1403	0.1401	0.1408	0.1419	–	
ρ_{BCP2} (au)[d]	–	–	–	–	0.1409	0.1408	0.1407	0.1412	0.1426	–	
r_{NNA} (Å)	–	0.8017	0.8016	0.8004	0.6688	0.6734	0.6790	0.6755	0.6865	–	

[a]XZ = cc-pVXZ, a-XZ = aug-cc-pVXZ, u-XZ = uncontracted cc-pVXZ, CVXZ = cc-pCVXZ, and 5Z-mod = cc-pV5Z modified. [b]CAS-SCF(6,8). [c]Calculation performed at the experimental geometry. [d]BCP1 is located between a boron atom and the NNA, while BCP2 is linking two NNAs.

Table 3. Equilibrium Bond Length (r_e), Harmonic Vibrational Frequency (ω), Total Energy (E_T), Number of Non-nuclear Attractors (NNAs), Atomic Charges (q_i), Densities at BCPs and NNAs (ρ), and the Distance between the Nearest Atom and the NNA (r_{NNA}) for the C_2 Molecule (Singlet State)[a]

	CCSD								CCSD(FU)	CAS[b]	
	DZ	TZ	a-TZ	u-TZ	QZ	a-QZ	u-QZ	5Z-mod	CVQZ	QZ	exp[46]
r_e (Å)	1.2662	1.2469	1.2468	1.2444	1.2421	1.2423	1.2421	1.2413	1.2425[c]	1.2425[c]	1.2425
ω (cm^{-1})	1861.5	1881.3	1877.4	1887.8	1892.7	1891.3	1891.9	1893.8	–	–	1855.0
$-E_T$(H)	75.7000	75.7496	75.7524	75.7545	75.7657	75.7668	75.7664	75.7692	75.8717	75.6432	
NNAs	0	1	1	1	2	2	2	2	2	0	
q_C (e)	0	0.397	0.392	0.437	0.362[e]	0.368[e]	0.377[e]	0.368[e]	0.361	0	
q_{NNA} (e)	–	−0.797	−0.786	−0.875	−0.362[e]	−0.371[e]	−0.378[e]	−0.368[e]	−0.362	–	
ρ_{NNA} (au)	–	0.3187	0.3192	0.3228	0.3235	0.3233	0.3235	0.3245	0.3225	–	
ρ_{BCP1} (au)[d]	–	0.3152	0.3159	0.3173	0.3229	0.3225	0.3225	0.3237	0.3217	–	
ρ_{BCP2} (au)[d]	–	–	–	–	0.3233	0.3231	0.3234	0.3245	0.3224	–	
r_{NNA} (Å)	–	0.6235	0.6234	0.6222	0.5337	0.5380	0.5472	0.5558	0.5443	–	

[a]XZ = cc-pVXZ, a-XZ = aug-cc-pVXZ, u-XZ = uncontracted cc-pVXZ, CVXZ = cc-pCVXZ, and 5Z-mod = cc-pV5Z modified. [b]CAS-SCF(8,8). [c]Calculation performed at the experimental geometry. [d]BCP1 is located between a carbon atom and the NNA, while BCP2 is linking two NNAs. [e]Obtained with AIMALL.

The data obtained for B_2 (Table 2) demonstrate that all CCSD calculations with a basis set of, at least, quadruple-ζ quality furnished two NNAs. The result from cc-pVDZ does not show any NNM. On the other hand, sets of triple-ζ quality yielded only one NNA at the center of the molecule, and its charge was nearly equal to the sum of those from the two NNMs found with larger sets. However, because CAS-SCF(6,8)/cc-pVQZ shows no NNA, one must try to include both dynamical and nondynamical (static) electron correlation at the highest possible level along with a large basis set (at least cc-pVQZ) to solve this issue. This molecule along with C_2 are the only cases among those chosen for more rigorous analyses in which the T1 diagnostic[49] is larger than 0.02 in CCSD calculations in their FC and FU variants. We also performed a CAS-SCF(6,26,RASSCF(0,0,2,18))/cc-pVQZ calculation at the experimental geometry, and two NNMs with similar characteristics to those obtained with CCSD and large basis sets (see Table S2, Supporting Information) were found again. The poor total energy values encountered in the calculations with cc-pVQZ and even larger active spaces that do not point to NNAs, CAS-SCF(6,28,RASSCF(0,0,2,20)) and CAS-SCF(6,34,RASSCF(0,0,2,26)) (see Table S2, Supporting Information), indicate that the convergence reached probably does not provide reliable results (Gaussian 03 generated a warning message during the last iteration informing that no convergence was encountered in wave functions). The electron density values at NNMs and at the BCP between them are similar, and differences observed are around 0.0001 and 0.0002 au. In addition, BCPs linking a NNA and a boron nucleus exhibit much smaller densities than ρ_{NNA}, resulting in a decrease from 0.0006 to 0.0008 au once two NNMs are present (see Table 2). Finally, the r_e and ω values given by CCSD with quadruple-ζ derived sets and cc-pV5Z-mod are in satisfactory agreement with experimental values,[46] with deviations of around 0.006–0.008 Å and 13–16 cm^{-1}, respectively.

The next molecule, C_2 (Table 3), is similar to B_2 regarding the features studied here. Again, CCSD calculations with quadruple-ζ and cc-pV5Z-mod sets show two NNMs, while none are obtained with CAS-SCF(8,8)/cc-pVQZ. However, investigating this problem more carefully, we discovered that multiconfigurational treatments that also include a larger fraction of dynamical correlation seem to recover the description with two NNAs for C_2. Although a CAS-SCF(8,26,RASSCF(4,2,2,18))/cc-pVQZ calculation still does not support NNMs, two NNAs are observed again in CAS-SCF(8,16), CAS-SCF(8,28,RASSCF(4,2,2,20)), and CAS-SCF-

dx.doi.org/10.1021/jp406992q | J. Phys. Chem. A 2013, 117, 10489−10496

Table 4. Equilibrium Bond Length (r_e), Harmonic Vibrational Frequency (ω), Total Energy (E_T), Number of Non-nuclear Attractors (NNAs), Atomic Charges (q_i), Densities at BCPs and NNAs (ρ), and the Distance between the Nearest Atom and the NNA (r_{NNA}) for the Na_2 Molecule (Singlet State)[a]

	CCSD								CCSD(FU)	
	DZ	TZ	a-TZ	u-TZ	QZ	a-QZ	u-QZ	5Z-mod	CVQZ	exp[46]
r_e (Å)	3.2046	3.1779	3.1778	3.1771	3.1773	3.1775	3.1773	3.1783	3.0789[b]	3.0789
ω (cm^{-1})	150.0	151.7	151.5	151.7	151.7	151.7	151.7	152.1	–	159.1
$-E_T$(H)	323.7311	323.7424	323.7424	323.7424	323.7439	323.7439	323.7439	323.7440	324.4273	
NNAs	0	1	1	1	1	1	1	1	0	
q_{Na} (e)	0	0.044	0.053	0.061	0.119	0.120	0.129	0.094[c]	0	
q_{NNA} (e)	–	−0.089	−0.107	−0.122	−0.238	−0.241	−0.259	−0.188[c]	–	
ρ_{NNA} (au)	–	0.0084	0.0085	0.0085	0.0085	0.0085	0.0085	0.0086	–	
ρ_{BCP} (au)	–	0.0084	0.0085	0.0085	0.0085	0.0085	0.0085	0.0086	–	
r_{NNA} (Å)	–	1.5890	1.5890	1.5886	1.5887	1.5888	1.5887	1.5892	–	

[a]XZ = cc-pVXZ, a-XZ = aug-cc-pVXZ, u-XZ = uncontracted cc-pVXZ, CVXZ = cc-pCVXZ, and 5Z-mod = cc-pV5Z modified. [b]Calculation performed at the experimental geometry. [c]Obtained with AIMALL.

Table 5. Equilibrium Bond Length (r_e), Harmonic Vibrational Frequency (ω), Total Energy (E_T), Number of Non-nuclear Attractors (NNAs), Atomic Charges (q_i), Densities at BCPs and NNAs (ρ), and the Distance between the Nearest Atom and the NNA (r_{NNA}) for the Si_2 Molecule (Triplet State)[a]

	CCSD								CCSD(FU)	CAS[b]	
	DZ	TZ	a-TZ	u-TZ	QZ	a-QZ	u-QZ	5Z-mod	CVQZ	QZ	exp[46]
r_e (Å)	2.2817	2.2542	2.2540	2.2534	2.2443	2.2443	2.2433	2.2408	2.246[c]	2.246[c]	2.246
ω (cm^{-1})	510.5	528.1	526.5	527.9	532.0	531.3	532.9	531.9	–	–	511.0
$-E_T$(H)	577.920	577.967	577.969	577.968	577.980	577.981	577.981	577.983	578.7227	577.8303	
NNAs	1	2	2	2	2	2	2	2	0	0	
q_{Si} (e)	0.572	0.516[e]	0.515[e]	0.489[e]	0.524	0.527	0.530	0.546	0	0	
q_{NNA} (e)	−1.144	−0.515[e]	−0.515[e]	−0.490[e]	−0.524	−0.528	−0.531	−0.547	–	–	
ρ_{NNA} (au)	0.0976	0.1013	0.1016	0.1015	0.1052	0.1050	0.1054	0.1054	–	–	
ρ_{BCP1} (au)[d]	0.0955	0.1012	0.1015	0.1014	0.1051	0.1049	0.1053	0.1051	–	–	
ρ_{BCP2} (au)[d]	–	0.1012	0.1014	0.1012	0.1050	0.1048	0.1052	0.1053	–	–	
r_{NNA} (Å)	1.1409	0.9409	0.9325	0.9182	0.9336	0.9379	0.9344	0.9768	–	–	

[a]XZ = cc-pVXZ, a-XZ = aug-cc-pVXZ, u-XZ = uncontracted cc-pVXZ, CVXZ = cc-pCVXZ, and 5Z-mod = cc-pV5Z modified. [b]CAS-SCF(8,8). [c]Calculation performed at the experimental geometry. [d]BCP1 is located between a silicon atom and the NNA, while BCP2 is linking two NNAs. [e]Obtained with AIMALL.

(8,34,RASSCF(2,2,2,26)) choices with the cc-pVQZ basis set (see Table S2, Supporting Information). Moreover, the latter calculation provides values in close agreement with the best results in Table 3. NNMs and the BCP between them show small differences in their electron densities, that is, around 0.0001 and 0.0002 au. On the other hand, the BCPs linking a carbon nucleus to a NNA show significantly smaller densities in comparison to ρ_{NNA} (results with two NNMs from Table 3 point to a decrease of roughly 0.0007−0.0010 au). Molecular properties from CCSD and cc-pV5Z-mod and quadruple-ζ variants for r_e and ω are in accordance with experimental data,[46] deviating by 0.0002−0.0012 Å and 36−39 cm^{-1}, respectively.

Table 4 shows the values obtained for Na_2. CCSD results point to a single NNA except by CCSD/cc-pVDZ. On the other hand, a NNM is no longer observed when a CCSD(FU)/cc-pCVQZ calculation is performed at the experimental geometry. However, because the experimental bond length in this molecule[46] is not correctly described by our CCSD(FC) calculations (deviations of 0.10 Å with quadruple-ζ or cc-pV5Z-mod sets), we performed another CCSD(FC)/cc-pVQZ calculation at this experimental distance, which yielded no NNA. The NNM in Na_2 is thus attributed to a poor representation of its geometry by these calculations. Such a conclusion is not surprising considering that the difference between ρ_{NNA} and ρ_{BCP} is almost null according to our CCSD(FC) investigations at optimized geometries (between 10^{-7} and 10^{-6} au with cc-pV5Z-mod and quadruple-ζ variations), so that slight disturbances may change the conclusions. Whether such NNA in Na_2 is real or not, it will have no easily detectable consequences because vibrational displacements are expected to smear this NNM out.

Results for Si_2 are in Table 5. All CCSD(FC) calculations with larger basis sets than cc-pVDZ furnish two NNAs. However, either a CV or a multiconfigurational description results in the absence of NNMs (they also disappear in a CCSD(FU)/cc-pVQZ calculation at the experimental bond length). The T1 diagnostic is larger than 0.02 in our CCSD(FC)/cc-pV5Z-mod calculation but decreases to only 0.01 as we change to CCSD(FU) with the same basis set. We have concluded that NNMs in the ground state of Si_2 are unphysical electron density features due to an incomplete electron correlation treatment. This is not in accordance with findings of Zhikol and co-workers,[14] as they attributed unphysical NNAs in the Si−Si bond of Si_2H_6 to deficiencies in the basis set. The influence of core valence correlation on NNM studies corroborates the arguments of Glaser and co-workers regarding the small electron density differences between such features and neighboring BCPs.[3] Despite this problem, other molecular properties from CCSD in combina-

dx.doi.org/10.1021/jp406992q | J. Phys. Chem. A 2013, 117, 10489−10496

Table 6. Equilibrium Bond Length (r_e), Harmonic Vibrational Frequency (ω), Total Energy (E_T), Number of Non-nuclear Attractors (NNAs), Atomic Charges (q_i), Densities at BCPs and NNAs (ρ), and the Distance between the Nearest Atom and the NNA (r_{NNA}) for the P_2 Molecule (Singlet State)[a]

	CCSD								CCSD(FU)	CAS[b]	
	DZ	TZ	a-TZ	u-TZ	QZ	a-QZ	u-QZ	5Z-mod	CVQZ	QZ	exp[46]
r_e (Å)	1.9217	1.8996	1.8997	1.8985	1.8894	1.8895	1.8890	1.8857	1.8934[c]	1.8934[c]	1.8934
ω (cm^{-1})	790.6	807.7	806.5	808.4	818.4	817.9	818.7	818.9	–	–	780.8
$-E_T$(H)	681.707	681.785	681.790	681.787	681.808	681.810	681.809	681.814	682.568	681.591	
NNAs	1	1	1	1	1	1	1	1	1	1	
q_P (e)	0.721	0.664	0.663	0.659	0.702	0.705	0.704	0.714	0.664	0.683	
q_{NNA} (e)	−1.442	−1.330	−1.329	−1.321	−1.405	−1.412	−1.409	−1.429	−1.330	−1.368	
ρ_{NNA} (au)	0.1668	0.1768	0.1774	0.1774	0.1842	0.1841	0.1844	0.1848	0.1835	0.1822	
ρ_{BCP} (au)	0.1612	0.1744	0.1750	0.1751	0.1815	0.1813	0.1816	0.1821	0.1811	0.1796	
r_{NNA} (Å)	0.9609	0.9498	0.9499	0.9493	0.9447	0.9448	0.9445	0.9429	0.9467	0.9467	

[a]XZ = cc-pVXZ, a-XZ = aug-cc-pVXZ, u-XZ = uncontracted cc-pVXZ, CVXZ = cc-pCVXZ, and 5Z-mod = cc-pV5Z modified. [b]CAS-SCF(10,8). [c]Calculation performed at the experimental geometry.

tion with cc-pV5Z-mod and quadruple-ζ sets, such as r_e and ω, are in agreement with experiment[46] (deviations of 0.002−0.005 Å and 20−22 cm^{-1} respectively).

Table 6 shows the values obtained for the last homonuclear molecule, P_2. All calculations consistently point to a single NNM at the middle of such a chemical bond. The best results from CCSD with cc-pV5Z-mod and quadruple-ζ variants indicate that the differences between ρ_{NNA} and ρ_{BCP} are around 0.0024 and 0.0028 au, the highest values detected in this work. Moreover, r_e and ω data calculated with cc-pV5Z-mod and quadruple-ζ derived sets are in satisfactory accordance with experiment[46] (deviations of 0.004−0.008 Å and 37−38 cm^{-1}, respectively).

Thus, our work is in general agreement with bond length windows for the appearance of NNMs in diatomic homonuclear molecules shown in the second figure of that work from Pendás et al.,[9] indicating that the promolecular model is a quite accurate tool to predict the existence of NNAs.

LiNa. Some authors have argued that NNMs are more likely to be found in heteronuclear molecules consisting of atoms of similar electronegativities;[3,10] therefore, we decided to test this hypothesis by choosing a molecule from this category containing elements that also show evidence of NNAs in their homonuclear counterparts. Table 7 exhibits the results for LiNa. All of the calculations performed at the experimental bond length[50] support a single NNM located closer to lithium than to sodium. Both alkaline metal atoms are positively charged (lithium is more positively charged than sodium by 0.15−0.21 e) and bonded to the pseudoatom associated with the basin containing this NNA. The ρ_{NNA} is larger than density values at the BCP between this attractor and lithium ($\rho_{BCP,Li}$) or sodium ($\rho_{BCP,Na}$) nuclei by 0.0001−0.0004 au. We also performed additional UCCSD(FU)/cc-pVQZ calculations with interatomic distances (r_{LiNa}) changing from 1 to 6 Å. One single NNA arose between 2.65 and 3.64 Å, while the other bond lengths studied resulted in no NNMs. Interestingly, as shown in Figure 1, the curve of molecular dipole moment values against these internuclear distances exhibits a change in the sign of its first derivative comprising all of the range in which one NNA is observed. Furthermore, the molecular quadrupole moment (zz component), not shown here, also has a maximum at 3.7 Å, soon after the NNM disappears. Curiously, a maximum was also detected by Penotti in the molecular quadrupole moment of Li_2 (3.383 Å) almost at the same internuclear distance in which one NNM splits into two (3.340 Å).[6] Figure 2 shows the

Table 7. Equilibrium Bond Length (r_e), Dipole Moment (μ), Total Energy (E_T), Number of Non-nuclear Attractors (NNAs), Atomic Charges (q_i), Densities at BCPs and NNAs (ρ), and the Distance between Lithium and the NNA ($r_{NNA,Li}$) for the LiNa Molecule (Singlet State)[a]

	CCSD	CAS[b]	CCSD(FU)	CCSD(FU)	
	QZ	QZ	QZ	CVQZ	exp[46,50]
r_e (Å)	2.885[c]	2.885[c]	2.885[c]	2.885[c]	2.885
μ (Debye)	0.917	0.915	0.746	0.581	0.463
$-E_T$(H)	169.3203	169.3229	169.3578	169.708	
NNAs	1	1	1	1	
q_{Na} (e)	0.350	0.342	0.315	0.286	
q_{Li} (e)	0.499	0.496	0.487	0.500	
q_{NNA} (e)	−0.850	−0.842	−0.802	−0.787	
ρ_{NNA} (au)	0.0112	0.0112	0.0114	0.0116	
$\rho_{BCP,Na}$ (au)	0.0108	0.0108	0.0112	0.0113	
$\rho_{BCP,Li}$ (au)	0.0111	0.0110	0.0111	0.0113	
$r_{NNA,Li}$ (Å)	1.2157	1.2237	1.2257	1.2350	

[a]QZ = cc-pVQZ and CVQZ = cc-pCVQZ. [b]CAS-SCF(8,11). [c]Calculation performed at the experimental geometry.

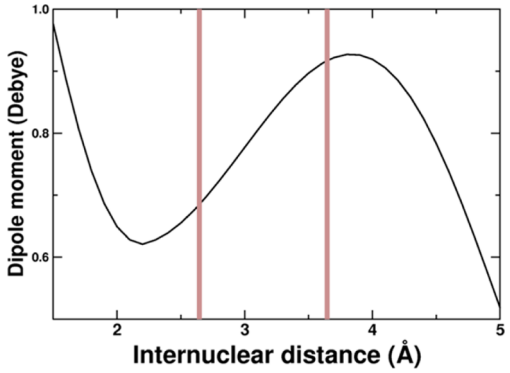

Figure 1. Molecular dipole moment values against interatomic distances obtained in UCCSD(FU)/cc-pVQZ calculations for LiNa (vertical lines delimit the region in which one NNM is observed). Sodium is placed at the positive end of the molecular axis.

density values at the NNA and BCPs. Indeed, a NNA remains until its density becomes equal to that associated with one BCP. Moreover, the order of density values is almost always the

dx.doi.org/10.1021/jp406992q | J. Phys. Chem. A 2013, 117, 10489−10496

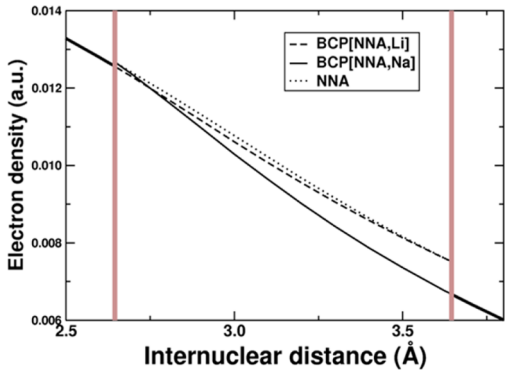

Figure 2. Electron density values against interatomic distances obtained in UCCSD(FU)/cc-pVQZ calculations for LiNa (vertical lines delimit the region in which one NNM is observed).

same, $\rho_{NNA} > \rho_{BCP,Li} > \rho_{BCP,Na}$, although an inversion between $\rho_{BCP,Li}$ and $\rho_{BCP,Na}$ is observed in a few points up to 2.7 Å.

Cioslowski[4] performed in 1990 an innovative analysis of the electron density in terms of Catastrophe Theory and discussed the bifurcation points observed in the phase diagram of Li_2. By using a similar approach for LiNa, as illustrated in Figure 3,

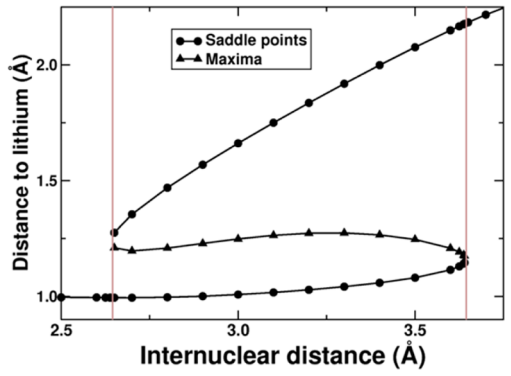

Figure 3. Diagram of distances between electron density features and the lithium nucleus according to bond length changes obtained in UCCSD(FU)/cc-pVQZ calculations for LiNa (vertical lines delimit the region in which one NNM is observed).

both NNM and BCP between this electron density feature and sodium split from a bifurcation point at an internuclear distance of 2.65 Å (this point is located 1.24 Å away from the lithium nucleus). The NNM disappears at another bifurcation point in which r_{LiNa} = 3.64 Å, merging with the BCP linking it to lithium (the distance from this point to the lithium nucleus is around 1.16 Å). Such a behavior is interpreted according to the QTAIM formalism as a donation of electronic charge from sodium to lithium, which is mediated by a pseudoatom. The charges from QTAIM are 0.48 e at r_{LiNa} = 2.64 Å, with lithium positively charged. Soon after the NNM had disappeared, at r_{LiNa} = 3.65 Å, the QTAIM charges became 0.27 e, with a positive charge on sodium instead. The negative charge ascribed to this pseudoatom at the equilibrium geometry of LiNa is almost equal to the charge amount transferred in this process (−0.8 e). Finally, the position of the NNM with respect to lithium remained almost unaltered (from 1.17 to 1.27 Å) during bond length variations in the entire range comprising a NNM (Figure 3). The overall conclusions drawn for LiNa were also confirmed in CCSD(FU)/cc-pCVQZ calculations performed for a few selected distances.

Finally, the distance window for observing NNAs obtained here for LiNa is almost exactly equal to the one that would be obtained by taking averages of initial and final points from results for Li_2 and Na_2, as seen in the second figure of the study from Pendás and co-workers (from 2.7 to 3.6 Å).[9] This is a strong argument in favor of the explanation for NNMs provided in that previous work. Hence, our investigation also supports that such electron density maxima are due to the atomic shell structure as reflected in the superposition of atomic electron densities with little disturbances caused by bond formation.

CONCLUSIONS

The best results shown here support that true NNMs are observed in ground-state electron densities of some homonuclear diatomic molecules at their equilibrium bond lengths: Li_2, B_2, C_2, and P_2. As far as we know, such features are also detected for the first time in a heteronuclear diatomic system at its equilibrium geometry, LiNa. One NNA was consistently found in Li_2, P_2, and LiNa, while B_2 and C_2 exhibited two NNMs in our most reliable treatments. Some calculations also pointed to NNAs in Si_2 and Na_2. However, a multiconfigurational treatment or the inclusion of CV led to the disappearance of those features in Si_2, indicating that an incomplete treatment of electron correlation is the cause of those unphysical NNMs. On the other hand, the poor description of equilibrium geometries given by CCSD(FC) optimized structures (deviations of 0.10 Å with respect to experiment) is the reason for the presence of NNAs in Na_2. The large differences in electron density values at the NNA and BCPs in P_2 suggest that crystals of this element might be excellent candidates for the experimental confirmation of NNMs.

Calculations performed in a range of internuclear distances for LiNa provided new evidence that molecular electric moments, such as dipole and quadrupole, are sensitive to the presence of NNMs. The molecular dipole moment presents a first derivative with respect to bond length changes with opposite sign in the region comprising a NNA, while the quadrupole moment shows a maximum almost at the same point in which the NNM disappears. The behavior observed during variations in internuclear distance for LiNa can be interpreted by the QTAIM formalism as resulting from some electronic charge exchange from sodium to lithium as r_{LiNa} increases (around 0.8 e), which is mediated by a pseudoatom.

ASSOCIATED CONTENT

Supporting Information

Additional tables from exploratory calculations in homonuclear diatomic molecules and multiconfigurational results for B_2 and C_2. This material is available free of charge via the Internet at http://pubs.acs.org.

AUTHOR INFORMATION

Corresponding Author

*E-mail: haiduke@iqsc.usp.br.

Notes

The authors declare no competing financial interest.

ACKNOWLEDGMENTS

The authors would like to acknowledge FAPESP for the financial support provided to this research (Grant Number

2010/18743-1). T.Q.T. also thanks FAPESP for a doctoral fellowship (Grant Number 2012/22143-5).

REFERENCES

(1) Besnainou, S.; Roux, M.; Daudel, R. Retour Sur Leffet de la Liaison Chimique sur la Densite Electronique. *C. R. Acad. Sci.* **1955**, *241*, 311−313.

(2) Bersuker, G. I.; Peng, C.; Boggs, J. E. The Nature of the Covalent Bond — The Existence and Origin of Nonnuclear Attractors. *J. Phys. Chem.* **1993**, *97*, 9323−9329.

(3) Glaser, R.; Waldron, R. F.; Wiberg, K. B. Origin and Consequences of the Nonnuclear Attractor in the Ab Initio Electron-Density Functions of Dilithium. *J. Phys. Chem.* **1990**, *94*, 7357−7362.

(4) Cioslowski, J. Nonnuclear Attractors in the Li_2 Molecule. *J. Phys. Chem.* **1990**, *94*, 5496−5498.

(5) Edgecombe, K. E.; Esquivel, R. O.; Smith, V. H., Jr.; Müller-Plathe, F. Pseudoatoms of the Electron-Density. *J. Chem. Phys.* **1992**, *97*, 2593−2599.

(6) Penotti, F. E. On the Eletronic Structure of Li_2 ($X^1\Sigma^+_g$) and Its Change with Internuclear Distance. *Int. J. Quantum Chem.* **2000**, *78*, 378−397.

(7) Gatti, C.; Fantucci, P.; Pacchioni, G. Charge-Density Topological Study of Bonding in Lithium Clusters. 1. Planar Li_N Clusters (N=4,5,6). *Theor. Chim. Acta* **1987**, *72*, 433−458.

(8) Cao, W. L.; Gatti, C.; MacDougall, P. J.; Bader, R. F. W. On the Presence of Nonnuclear Attractors in the Charge-Distributions of Li and Na Clusters. *Chem. Phys. Lett.* **1987**, *141*, 380−385.

(9) Pendás, A. M.; Blanco, M. A.; Costales, A.; Mori-Sánchez, P.; Luaña, V. Non-Nuclear Maxima of the Electron Density. *Phys. Rev. Lett.* **1999**, *83*, 1930−1933.

(10) Costales, A.; Blanco, M. A.; Pendás, A. M.; Mori-Sánchez, P.; Luaña, V. Universal Features of the Topological Bond Properties of the Electron Density. *J. Phys. Chem. A* **2004**, *108*, 2794−2801.

(11) Friis, J.; Madsen, G. K. H.; Larsen, F. K.; Jiang, B.; Marthinsen, K.; Holmestad, R. Magnesium Comparison of Density Functional Theory Calculations with Electron and X-ray Diffraction Experiments. *J. Chem. Phys.* **2003**, *119*, 11359−11366.

(12) Madsen, G. K. H.; Blaha, P.; Schwarz, K. On the Existence of Non-Nuclear Maxima in Simple Metals. *J. Chem. Phys.* **2002**, *117*, 8030−8035.

(13) Luaña, V.; Mori-Sánchez, P.; Costales, A.; Blanco, M. A.; Pendás, A. M. Non-Nuclear Maxima of the Electron Density on Alkaline Metals. *J. Chem. Phys.* **2003**, *119*, 6341−6350.

(14) Zhikol, O. A.; Oshkalo, A. F.; Shishkin, O. V.; Prezhdo, O. V. Non-Nuclear Attractor on Si−Si Bond in Quantum-Chemical Modeling as Basis Set Inadequacy. *Chem. Phys.* **2003**, *288*, 159−169.

(15) Tognetti, V.; Joubert, L. On the Influence of Density Functional Approximations on Some Local Badeŕs Atoms-in-Molecules Properties. *J. Phys. Chem. A* **2011**, *115*, 5505−5515.

(16) Bader, R. F. W.; Platts, J. A. Characterization of an F-Center in an Alkali Halide Cluster. *J. Chem. Phys.* **1997**, *20*, 8545−8553.

(17) Platts, J. A.; Overgaard, J.; Jones, C.; Iversen, B. B.; Stasch, A. First Experimental Characterization of a Non-nuclear Attractor in a Dimeric Magnesium(I) Compound. *J. Phys. Chem. A* **2011**, *115*, 194−200.

(18) Bader, R. F. W. Atoms in Molecules. *Acc. Chem. Res.* **1985**, *18*, 9−15.

(19) Bader, R. F. W. Atoms in Molecules: A Quantum Theory; Clarendon Press: Oxford, U.K., 1990.

(20) Frisch, M. J.; Trucks, G. W.; Schlegel, H. B.; Scuseria, G. E.; Robb, M. A.; Cheeseman, J. R.; Montgomery, J. A., Jr.; Vreven, T.; Kudin, K. N.; Burant, J. C.; et al. *Gaussian 03*, revision D.02; Gaussian, Inc.: Wallingford, CT, 2004.

(21) Cioslowski, J.; Piskorz, P.; Rez, P. Accurate Analytical Representations of the Core-Electron Densities of the Elements 3 through 118. *J. Chem. Phys.* **1997**, *106*, 3607−3612.

(22) Cioslowski, J.; Stefanov, B. B. Analytical Derivatives of Atomic Zero-Flux Surfaces and Properties of Atoms in Molecules with Respect to External Perturbations. *J. Chem. Phys.* **1996**, *105*, 8741−8747.

(23) Cioslowski, J. Theory of Response Properties of Atoms in Molecules. *Mol. Phys.* **1996**, *88*, 621−629.

(24) Cioslowski, J.; Piskorz, P. Properties of Atoms in Molecules from Valence-Electron Densities Augmented with Core-Electron Contributions. *Chem. Phys. Lett.* **1996**, *255*, 315−319.

(25) Cioslowski, J.; Stefanov, B. B. Symmetry Handling in Calculations of Properties of Atoms in Molecules. *Chem. Phys. Lett.* **1996**, *256*, 449−453.

(26) Cioslowski, J.; Stefanov, B. B. Variational Determination of the Zero-Flux Surfaces of Atoms in Molecules. *Mol. Phys.* **1995**, *84*, 707−716.

(27) Stefanov, B. B.; Cioslowski, J. An Efficient Approach to Calculation of Zero-Flux Atomic Surfaces and Generation of Atomic Integration Data. *J. Comput. Chem.* **1995**, *16*, 1394−1404.

(28) Cioslowski, J.; Nanayakkara, A. A New Robust Algorithm for Fully Automated-Determination of Attractor Interaction Lines in Molecules. *Chem. Phys. Lett.* **1994**, *219*, 151−154.

(29) Cioslowski, J.; Nanayakkara, A.; Challacombe, M. Rapid Evaluation of Atomic Properties with Mixed Analytical Numerical Integration. *Chem. Phys. Lett.* **1993**, *203*, 137−142.

(30) Cioslowski, J. An Efficient Evaluation of Atomic Properties Using a Vectorized Numerical-Integration with Dynamic Thresholding. *Chem. Phys. Lett.* **1992**, *194*, 73−78.

(31) Cioslowski, J.; Mixon, S. T. Topological Properties of Electron-Density in Search of Steric Interactions in Molecules — Electronic Structure Calculations on Ortho-Substituted Biphenyls. *J. Am. Chem. Soc.* **1992**, *114*, 4382−4387.

(32) Cioslowski, J.; Surján, P. R. An Observable Based Interpretation of Electronic Wave-Functions — Application to Hypervalent Molecules. *J. Mol. Struct.: THEOCHEM* **1992**, *87*, 9−33.

(33) Cioslowski, J.; Mixon, S. T. Covalent Bond Orders in the Topological Theory of Atoms in Molecules. *J. Am. Chem. Soc.* **1991**, *113*, 4142−4145.

(34) Cioslowski, J. Isopycnic Orbital Transformations and Localization of Natural Orbitals. *Int. J. Quantum Chem.* **1990**, *S24*, 15−28.

(35) Keith, T. A. *AIMAll*, version 12.08.21; TK Gristmill Software: Overland Park, KS, 2012 (aim.tkgristmill.com).

(36) Dunning, T. H., Jr. Gaussian-Basis Sets for Use in Correlated Molecular Calculations. 1. The Atoms Boron through Neon and Hydrogen. *J. Chem. Phys.* **1989**, *90*, 1007−1023.

(37) Prascher, B. P.; Woon, D. E.; Peterson, K. A.; Dunning, T. H., Jr.; Wilson, A. K. Gaussian Basis Set for Use in Correlated Molecular Calculations. VII. Valence, Core-Valence, and Scalar Relativistic Basis Sets for Li, Be, Na, and Mg. *Theor. Chem. Acc.* **2011**, *128*, 69−82.

(38) Woon, D. E.; Dunning, T. H., Jr. Gaussian-Basis Sets for use in Correlated Molecular Calculations. 3. The Atoms Aluminum through Argon. *J. Chem. Phys.* **1993**, *98*, 1358−1371.

(39) Kendall, R. A.; Dunning, T. H., Jr.; Harrison, R. J. Electron-Affinities of the 1st-Row Atoms Revisited — Systematic Basis-Sets and Wave-Functions. *J. Chem. Phys.* **1992**, *96*, 6796−6806.

(40) Woon, D. E.; Dunning, T. H., Jr. Gaussian-Basis Sets for use in Correlated Molecular Calculations. 4. Calculation of Static Electric Response Properties. *J. Chem. Phys.* **1994**, *100*, 2975−2988.

(41) Koput, J.; Peterson, K. A. Ab Initio Potential Energy Surface and Vibrational−Rotational Energy Levels of $X^2\Sigma^+$ CaOH. *J. Phys. Chem. A* **2002**, *106*, 9595−9599.

(42) Woon, D. E.; Dunning, T. H., Jr. Gaussian Basis Sets for Use in Correlated Molecular Calculations. V. Core−Valence Basis Sets for Boron through Neon. *J. Chem. Phys.* **1995**, *103*, 4572−4585.

(43) Feller, D. Unpublished work, 2013.

(44) Feller, D. The Role of Databases in Support of Computational Chemistry Calculations. *J. Comput. Chem.* **1996**, *17*, 1571−1586.

(45) Schuchardt, K. L.; Didier, B. T.; Elsethagen, T.; Sun, L.; Gurumoorthi, V.; Chase, J.; Li, J.; Windus, T. L. Basis Set Exchange: A Community Database for Computational Sciences. *J. Chem. Inf. Model.* **2007**, *47*, 1045−1052.

(46) Haynes, W. M., Ed. *CRC Handbook of Chemistry and Physics*, 91st ed., Internet version; CRC Press/Taylor and Francis: Boca Raton, FL, 2011.
(47) Huber, K. P.; Herzberg, G. Constants of Diatomic Molecules (data prepared by J. W. Gallagher and R. D. Johnson, III). In *NIST Chemistry WebBook*, NIST Standard Reference Database Number 69; Linstrom, P. J., Mallard, W. G., Eds.; National Institute of Standards and Technology: Gaithersburg, MD; http://webbook.nist.gov (retrieved April 30, 2013).
(48) Bondybey, V. E. Electronic Structure and Bonding of Be_2. *Chem. Phys. Lett.* **1984**, *109*, 436−441.
(49) Lee, T. J.; Taylor, P. R. A Diagnostic for Determining the Quality of Single-Reference Electron Correlation Methods. *Int. J. Quantum Chem., Quantum Chem. Symp.* **1989**, *S23*, 199−207.
(50) Engelke, F.; Ennen, G.; Meiwes, K. H. Laser Induced Fluorescence Spectroscopy of NaLi in Beam and Bulk. *Chem. Phys.* **1982**, *66*, 391−402.